Bearing Behavior and Post-Grouting Mechanisms of Large-Diameter Bored Piles in Clay–Silt Interbedded Strata

Manyi Liu[a*], Jiaxin Lu[a], Jianjun Zhang[a], Chuang Sun[a], Weixiang Zhou[b], Min Liu[b]

[a] School of Civil Engineering, Liaoning Technical University, Fuxin 123000, China
[b] China Railway Design Corporation, Tianjin 300308, China

*13114916693@163.com

Abstract. The clay–silt interbedded stratum exhibits complex structural features and significant variations in soil permeability. Accumulated sediment at the pile tip and disturbance along the pile–soil interface are common problems, which often restrict the mobilization of end resistance, lead to uneven distribution of shaft resistance, and cause the load-bearing performance of cast-in-place piles to deviate from design expectations. To evaluate the practical reinforcement effect of post-grouting in this type of strata, this study relies on the pile foundation project of the main tower of the Jinwei Railway Dongying Yellow River Bridge. Two self-balanced static load tests were performed on the same test pile before and after post-grouting, and the influence of grouting on pile-end resistance, shaft resistance, and load-transfer characteristics was systematically analyzed.

Test results show that pile-end resistance increases significantly after grouting, rising from 12,252 kN before grouting to 26,194 kN after grouting, an increase of more than 100%. Shaft resistance also increases at all depth segments, with the shallow layers showing the most prominent improvement, while the middle and deep layers exhibit relatively stable enhancement. Grouting improves the overall stiffness of the load–displacement curve, and the ultimate bearing capacity increases from 82,442 kN before grouting to 115,545 kN after grouting. The load-transfer mode also changes markedly, shifting from a "shallow-layer-dominated" pattern before grouting to a "multi-layer collaborative" pattern afterward. These findings indicate that post-grouting can effectively improve the pile–soil interface conditions in interbedded strata and enhance the bearing efficiency of large-diameter cast-in-place piles, providing a reference for the design and construction of pile foundations in similarly complex geological conditions.

Keywords: large-diameter cast-in-place piles; post-grouting; clay–silt interbedded strata; pile-end resistance; shaft resistance; load transfer mechanism

1 Introduction

Large-diameter bored cast-in-place piles are widely used in high-speed railway foundations and long-span river-crossing bridges due to their high bearing capacity and

S. Sing et al. (eds.), *Proceedings of the 2025 7th International Conference on Civil Architecture and Urban Engineering (ICCAUE 2025)*, Atlantis Highlights in Engineering 43,
https://doi.org/10.2991/978-94-6239-682-1_20

strong adaptability. Their vertical load-bearing performance is directly associated with the overall safety and serviceability of the structural system. In clay–silt interbedded strata, however, the engineering behavior of the ground becomes highly complex. The loose and highly permeable silt layers, together with the low-permeability and highly compressible silty clay layers, make it difficult to remove sediment at the pile tip and maintain stable pile–soil bonding. These factors often lead to considerable variability in the mobilization of end resistance and shaft resistance along the pile length [1–3], reflecting the high sensitivity of load transfer to stratigraphic heterogeneity.

Post-grouting has been increasingly adopted as an effective technique to improve pile performance by densifying the sediments at the pile tip, strengthening the pile–soil interface, and forming grout-induced cemented zones around the pile. Recent studies have consistently shown that post-grouting can significantly increase pile-end resistance, enhance shaft resistance, and improve the continuity of load transfer along the pile body under various soil conditions [1–6]. The magnitude and depth-wise distribution of these improvements are strongly governed by grout diffusion behavior, permeability contrasts between layers, and the development of interface bonding, which together control the mobilization of shaft resistance during loading [4–6].

International research further reveals that post-grouting raises deep-soil stiffness, increases effective stress, and promotes multi-layer collaborative load transfer—mechanisms that are particularly relevant in layered geological systems such as clay–silt interbedded formations [7–9].

In such strata, load transfer is influenced simultaneously by layers exhibiting different stiffness, drainage characteristics, and structural features; thus, the strengthening effects of post-grouting vary substantially with depth and require validation through full-scale field testing [9–10].

Therefore, evaluating post-grouting behavior in interbedded strata must consider both the macroscopic improvement in bearing capacity and the evolution of the load-transfer mechanism with depth—an aspect emphasized in recent experimental and numerical studies [9–10].

Given these considerations, this study investigates the effect of post-grouting on a large-diameter bored pile at the main tower foundation of the Dongying Yellow River Bridge along the Jinwei Railway. Two self-balanced static load tests were carried out on the same test pile (SZ1) before and after post-grouting. By comparing the development of pile-end resistance, shaft resistance, and the overall load-transfer behavior under both conditions, this study clarifies the enhancement mechanisms that govern pile–soil interaction in clay–silt interbedded strata and provides field-based evidence of the effectiveness of post-grouting for large-diameter bored piles under complex layered geological conditions.

2 Experimental Program

The test site is located in the alluvial plain of the Yellow River, where the subsurface strata consist of alternating layers of silt, fine sand, and silty clay, forming a typical interbedded sedimentary structure. The fine sand layers exhibit high permeability and

loose structure, whereas the silty clay layers are characterized by low permeability and dense structure. These stratigraphic characteristics make the removal of sediment at the pile tip and the maintenance of the pile–soil interface critical issues during construction. As shown in Figure 1, the load cell was installed within the reinforcement cage of the test pile to realize the self-balanced static load test and to monitor the load-transfer response of different pile segments.

Fig. 1. Schematic Diagram of the Load Cell and Its Connection to the Reinforcement Cage in the Test Pile

Table 1 presents the embedment elevations and relative positions of the upper and lower load cells in Test Pile 1, which provide the basis for identifying the load-transfer characteristics of the upper and lower pile sections during loading.

Table 1. Embedment Elevation of the Load Cell in Test Pile 1

Positions and Elevations of Load Cells (m)		Positions and Elevations of the Load Cells (m)
Elevation of the Upper Load Cell	-49.21	2×40000
Distance from the Pile Tip	65.383	
Elevation of the Lower Load Cell	-79.01	2×43000
Distance from the Pile Tip	35.583	

3 Performance of Post-Grouted Piles and Analysis of Load-Transfer Mechanisms

3.1 Characteristics of Bearing Capacity and Load–Displacement Behavior

As shown in Fig. 2, the load–displacement curve of the pile before grouting exhibits a softening trend, with displacement increasing rapidly during the high-load stage, indicating insufficient densification at the pile tip and inadequate bonding along the pile–soil interface. As shown in Fig. 3, after grouting, the overall stiffness of the load–

displacement curve increases significantly, and the rate of displacement growth under high loads is markedly reduced, demonstrating improvements in the stress conditions at both the pile tip and the pile shaft. The ultimate bearing capacity of the test pile increases from 82,442 kN to 115,545 kN, representing an increase of approximately 40%.

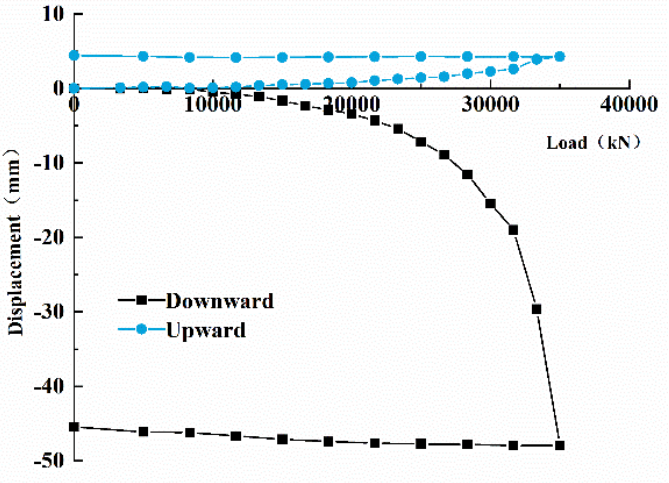

(a) Lower Load Cell Response of Test Pile SZ1 Before Grouting

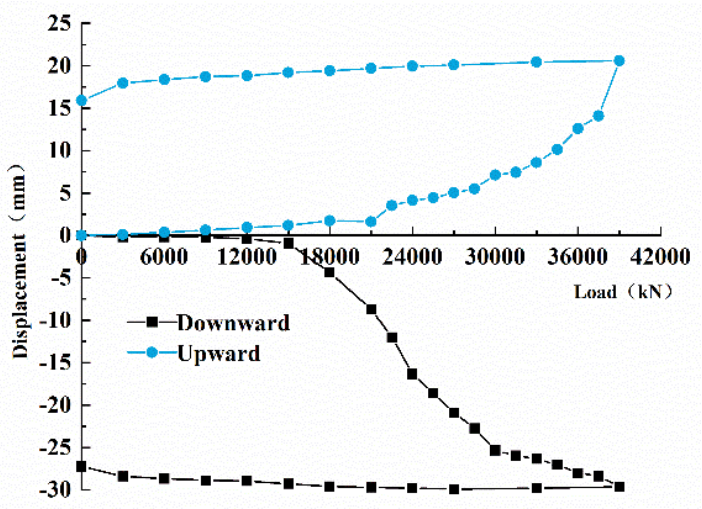

(b) Upper Load Cell of Test Pile SZ1 Before Grouting

Fig. 2. Load–Displacement Curve of SZ1 Before Grouting

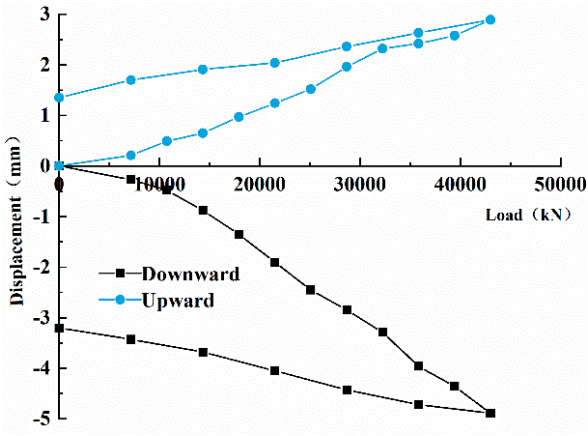

(a) Lower Load Cell of Test Pile SZ1 After Grouting

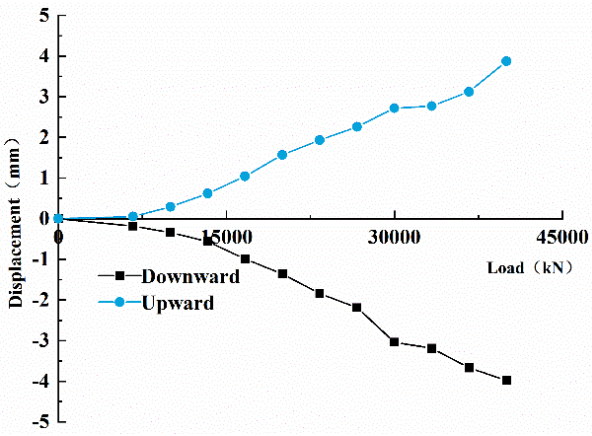

(b) Upper Load Cell of Test Pile SZ1 After Grouting

Fig. 3. Load–Displacement Curve of SZ1 After Grouting

3.2 Layered Enhancement of Shaft Resistance

As shown in Fig. 4, the magnitude of shaft resistance improvement is strongly controlled by the permeability of the soil layers. In the shallow silt–fine sand segment, where permeability is relatively high and grout diffusion is sufficient, the enhancement of shaft resistance is the most pronounced, reaching approximately 45.5%. In the middle fine sand segment, the soil structure is uniform and the reinforced zone exhibits good continuity, resulting in an increase of about 20%. In the deeper silty clay segment, the low permeability limits grout diffusion, and the improvement in shaft resistance is relatively modest (around 14%), although the overall enhancement trend remains evident.

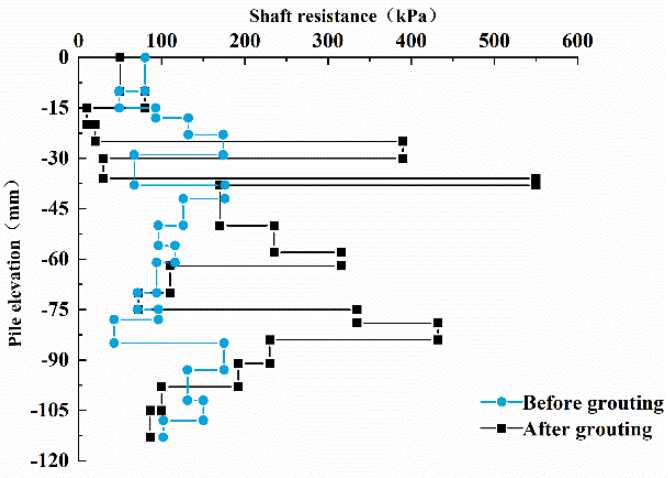

Fig. 4. Distribution of Shaft Friction Along Depth at Ultimate Load for Each Segment of SZ1 Before and After Grouting

3.3 Improvement of Pile-End Resistance and Mechanism Analysis

As shown in Fig. 5, before grouting, the development of shaft resistance exhibits a clear depth-dependent pattern as the pile–soil relative displacement increases. In the upper silt–fine sand zone, where the soil structure is relatively loose, shaft resistance is mobilized rapidly under small displacements, reaching peak values of 55–70 kPa followed by slight softening. In the middle dense fine-sand layer, shaft resistance increases smoothly with displacement, the curve maintains a stable slope without softening, and peak values of 80–90 kPa indicate strong interface bonding and efficient load transfer. In the lower segment near the bearing stratum, the initial shaft resistance is low but rises sharply to above 100 kPa when the displacement reaches 8–10 mm, showing noticeable hysteresis and suggesting that the deep interface had not fully mobilized its capacity before grouting but retains significant potential for further enhancement.

The pile-end resistance exhibits the greatest increase, rising from 12,252 kN to 26,194 kN, with an improvement of more than 100%. This significant enhancement is primarily attributed to the densification of sediment at the pile tip, the rearrangement of particles within the bearing stratum, and the cemented structure formed by grout solidification, all of which substantially increase the strength and deformation modulus of the soil at the pile end.

To link the observed improvement in base resistance with soil–mechanics principles, the ultimate toe resistance can be expressed as:

$$Q_b = q_{bu} A_b \tag{1}$$

$$q_{bu} = c' N_c + \sigma'_{v0} N_q + 0.5 \gamma' B N_\gamma \tag{2}$$

The bearing-capacity factors N_q and N_γ increase markedly with the effective friction angle ϕ', for example:

$$N_q = e^{\pi \tan \phi'} \cdot \tan^2(45^\circ + \phi'/2) \tag{3}$$

$$N_\gamma = (N_q - 1)\tan \phi' \tag{4}$$

In this study, post-grouting increased the toe resistance from 12,252 kN to 26,194 kN (>100%). This indicates that grouting densified the sediment at the pile base, rearranged particle structure, and formed a cemented bulb with higher stiffness, which effectively increased the equivalent ϕ', and thereby enhanced N_q, N_γ, and q_{bu}, producing the substantial gain in end-bearing capacity.

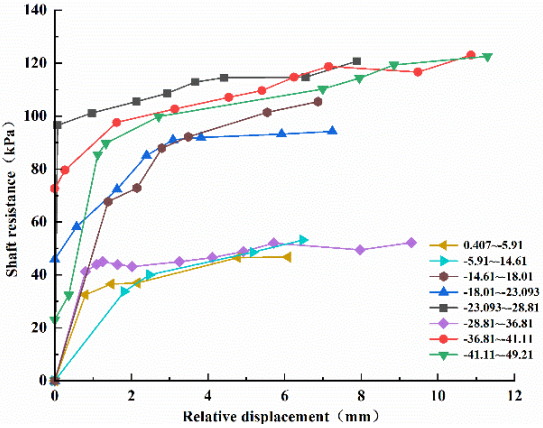

(a)Upper Section of Pile SZ1

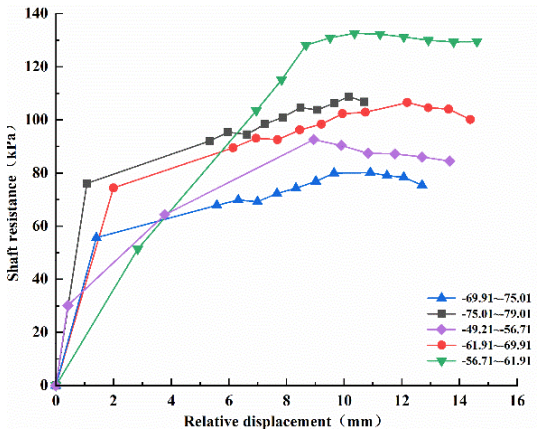

(b) Middle Section of Pile SZ1

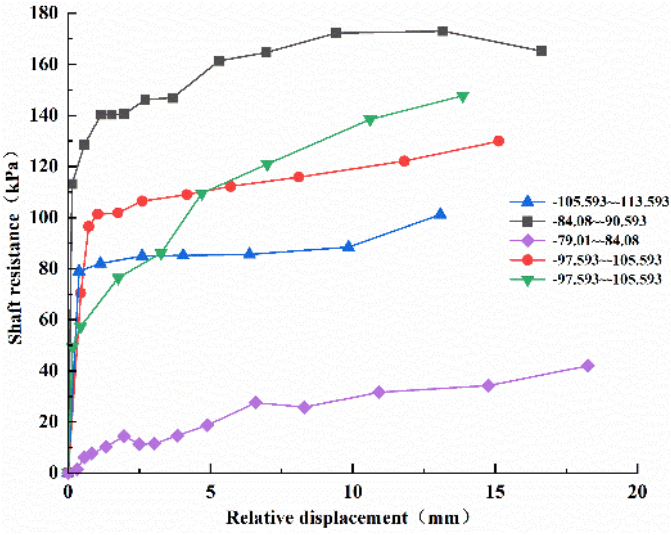

(c) Lower Section of Pile SZ1

Fig. 5. Shaft Friction–Displacement Curves of Different Segments of SZ1 Before Grouting

3.4 Changes in the Load-Transfer Mechanism

After grouting, the shaft resistance of all pile sections increases significantly, exhibiting a clear depth-dependent enhancement pattern. In the upper silt–fine sand zone, the peak shaft resistance rises from 55–70 kPa to 85–100 kPa, with a steeper curve slope and reduced softening, indicating substantial improvement of the interface conditions. In the middle dense fine-sand layer, shaft resistance increases to 95–110 kPa, representing the largest enhancement (exceeding 25%), which reflects effective grout penetration and markedly improved interface shear capacity. In the lower section near the bearing stratum, the peak resistance exceeds 120 kPa, and the curve tends toward saturation with a steeper initial slope. This demonstrates strengthened deep-interface conditions, enabling considerable shaft resistance to be mobilized at an early loading stage and significantly enhancing the contribution of deep soil layers to load transfer.

As shown in Fig. 6, before grouting, the load was mainly carried and released rapidly within the shallow layers, while the middle and deep layers contributed insufficiently to the overall bearing behavior. After grouting, improvements at both the pile–soil interface and the pile tip led to a significant increase in shaft resistance in the middle and deep layers. As a result, load transfer along the pile depth became more continuous, forming a “multi-layer collaborative” bearing pattern. The contribution of deeper soil layers increased markedly, resulting in a more stable and effective load-transfer system.

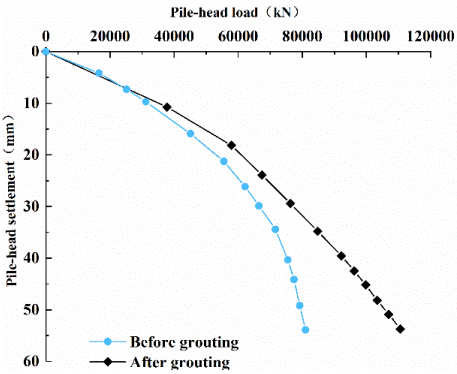

Fig. 6. Equivalent Converted Load–Displacement Curves at the Pile Head of SZ1 Before and After Grouting

4 Conclusions

(1) Post-grouting markedly enhances the vertical bearing capacity of large-diameter cast-in-place piles. The end–side combined grouting scheme delivers the greatest improvement, raising the ultimate bearing capacity by approximately 40%.

(2) Shaft resistance increases with a distinct stratified pattern: shallow layers exhibit the most significant enhancement, middle layers maintain stable improvement, and deep layers—though limited by low permeability—still demonstrate measurable gains.

(3) Pile-end resistance increases by more than 100%, primarily due to the densification of the bearing stratum and the substantial enhancement of its stiffness, which collectively form the main sources of the overall bearing-capacity improvement.

(4) Grouting modifies the load-transfer mechanism from a shallow-dominated pattern to a multi-layer collaborative mode, significantly strengthening pile–soil interaction and providing practical guidance for the design and parameter optimization of post-grouted piles in interbedded soil strata.

References

1. Wang, W., Wan, Z., Dai, G., & Liu, H. (2024). Experimental study on vertical bearing behavior of post-grouted large-diameter bored piles. *Journal of Building Structures*, 45(4), 155–165.
2. Li, G. (2024). Study on bearing capacity of post-grouted bored piles based on static load tests. *Northern Architecture*, 9(5), 31–35.
3. Jiang, S. (2023). Bearing behavior of post-grouted bored piles in sand layers of the Yellow River alluvial plain. *Railway Construction Technology*, 1–5.
4. Rao, S., Wan, Z., Luo, Z., & Dai, G. (2022). Experimental study on bearing behavior of large-diameter post-grouted rock-socketed piles in weathered rock. *Journal of Building Structures*, 43(S1), 287–295.
5. Xu, Y., Wan, Z., Dai, G., et al. (2021). Long-term bearing performance of post-grouted bored piles. *Journal of Building Structures*, 42(4), 139–146.

6. Duan, C., Wan, Z., Dai, G., et al. (2025). Vertical bearing behavior of post-grouted rock-socketed piles in coral-reef limestone. *Chinese Journal of Rock Mechanics and Engineering*, 44(3), 721–736.
7. Wu, G., Yu, W., Zuo, J., et al. (2020). Experimental and theoretical investigation on rock–coal composite systems. *International Journal of Mining Science and Technology*, 30(6), 759–768.
8. Ma, Q., Tan, Y., Liu, X., et al. (2021). Mechanical and energy characteristics of composite samples. *Environmental Earth Sciences*, 80, 309.
9. Li, T., Chen, G., Li, Y., et al. (2022). Progressive instability characteristics of composite geomaterials. *Geotechnical and Geological Engineering*, 1–14.
10. Yu, W., Wang, B., Zi, X., et al. (2024). Elastoplastic coupling analysis of surrounding rock–prestressed anchor systems. *Tunnelling and Underground Space Technology*, 143, 105491.